

# Quantum Model-Discovery

Niklas Heim<sup>1,2</sup>, Atiyo Ghosh<sup>1</sup>, Oleksandr Kyriienko<sup>1,3</sup>, and Vincent E. Elfving<sup>1</sup>

<sup>1</sup>Qu & Co B.V., PO Box 75872, 1070 AW, Amsterdam, The Netherlands

<sup>2</sup>Artificial Intelligence Center, Czech Technical University, Prague, CZ 120 00

<sup>3</sup>Department of Physics and Astronomy, University of Exeter, Stocker Road, Exeter EX4 4QL, United Kingdom

November 12, 2021

## Abstract

Quantum computing promises to speed up some of the most challenging problems in science and engineering. Quantum algorithms have been proposed showing theoretical advantages in applications ranging from chemistry to logistics optimization. Many problems appearing in science and engineering can be rewritten as a set of differential equations. Quantum algorithms for solving differential equations have shown a provable advantage in the fault-tolerant quantum computing regime, where deep and wide quantum circuits can be used to solve large linear systems like partial differential equations (PDEs) efficiently. Recently, variational approaches to solving non-linear PDEs also with near-term quantum devices were proposed. One of the most promising general approaches is based on recent developments in the field of scientific machine learning for solving PDEs. We extend the applicability of near-term quantum computers to more general scientific machine learning tasks, including the discovery of differential equations from a dataset of observations.

We use differentiable quantum circuits (DQCs) to solve equations parameterized by a library of operators, and perform regression on a combination of data and equations. Our results show a promising path to quantum model discovery (QMoD), on the interface between classical and quantum machine learning approaches. We demonstrate successful parameter inference and equation discovery using QMoD on different systems including a second-order, ordinary differential equation and a non-linear, partial differential equation.

## 1 Introduction

Recent advances in automatic differentiation in classical computers have led to novel machine learning based approaches to scientific computing, often referred to as scientific machine learning. For example, incorporating neural networks into classical ordinary differential equation solvers [1], or manipulating neural network derivatives towards prescribed differential equations [2]. The applications of such techniques have included inference of unobserved states [3], inference of differential equation parameters [4] and approaches to solve differential equations [2], or discover differential equations from observed data [5]. Such methods depend on machine learning techniques and are often end-to-end differentiable.

---

Corresponding author: [vincent.elfving@quandco.com](mailto:vincent.elfving@quandco.com)

Recent progress in automatic differentiation on quantum computers [6–14] introduce the prospect of extending recent classical results in scientific machine learning to a quantum setting. These techniques have already led to quantum methods of solving differential equations [15] which are analogous to methods involving classical neural networks [2]. However, the existence of quantum automatic differentiation opens the door to further cross pollination between classical scientific machine learning and quantum computing.

In this work, we target an important task in scientific machine learning and modelling in general; while many systems can be modelled using differential equations, and their solving constitutes an important task in phenomenological understanding, in many practical settings these equations are not (fully) known. In such cases, one may have access to observations on some target system, and some initial idea of the dynamics.

Parameter inference in differential equations is an essential part of combining theoretical models with empirical observations. Oftentimes a given mechanism might be speculated for an observed process in the form of a differential equation, but whose coefficients must be inferred from empirical observations.

Model discovery (often referred to as equation discovery) tries to find a mathematical expression that describes a given dataset. We specifically tackle the problem of discovering a differential equation only from observations of a given system. By *discovery* we mean an interpretable (i.e. human readable) model in symbolic form, which can be converted directly into a differential equation.

This task is generally not suited for treatment by finite-differencing techniques, since such applications require many repeated simulations. Instead, to treat such a case of mixture of equation solving and model discovery efficiently, we generalize two techniques from the realm of classical scientific machine learning to a quantum setting: differential equation parameter inference and differential equation model discovery. We also highlight conceptual similarities between scientific machine learning and quantum computing that might point to further research avenues.

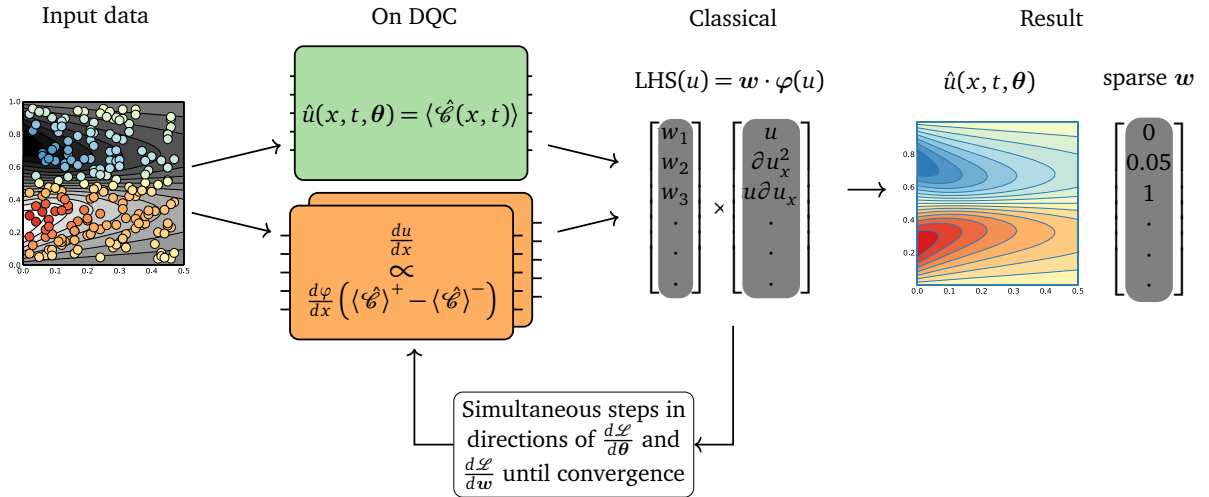


Figure 1: Schematic of the quantum model discovery approach (QMoD). The solution to the differential equation is represented by a (quantum) universal function approximator (UFA) with variational angles  $\theta$ . Both the forward pass and the gradients w.r.t. parameters  $\theta$  as well as gradients w.r.t. inputs (in this example  $x$  and  $t$ ) are computed on the DQC. QMoD learns a sparse  $w$  which chooses only a few functions from the library of basis functions  $\varphi$ . Gradients w.r.t. the basis function coefficients  $w$  are computed classically. The figure depicts how QMoD learns the solution  $\hat{u}$  and a sparse  $w$  that only contains the two basis functions that are necessary to represent the input data from Burgers’ equation.

We first recap how quantum computers can be used to represent solutions to differential equations via variational procedures. Then we introduce the broad field of scientific machine learning and propose how quantum computers can be used for these nascent developments.

**Universal Function Approximation on Quantum Devices.** For the past several decades, the number of transistors on a similarly-sized integrated chip doubles roughly every two years or so; this is known as Moore’s law [16] and is an observation rather than a guarantee. In the past 10 years or so, a shift has started where more computational power can only be reached by parallelization rather than minimization or increasing clock speeds [17]; this is due to the fundamental limitations of electronics. While alternative classical hardware proposals are interesting, such as photonic [18] or biological [19] computers, these will quickly hit a wall of unsustainable exponential speed increase too.

A completely different compute paradigm, quantum computing, has existed for over 4 decades but has only recently emerged as a truly promising next stage of computational hardware developments. Large corporate players including IBM [20] and Google [21], as well as a range of startups including IonQ, Pasqal, Xanadu and Rigetti, are investing large amounts of funding for such hardware, and with that the development of quantum computational algorithms has gotten a resurgence from the initial fundamental algorithms like Shor’s [22] or Grover’s [23] algorithms. Some of the promising areas where universal fault-tolerant quantum computing hardware could show a possible quantum advantage include quantum chemistry simulations [24, 25] and quantum-enhanced machine learning [26].

Recent algorithm developments have also focused on compatibility with current noisy intermediate scale quantum (NISQ) devices [27]. Such algorithms are typically variational in nature, and are being applied to fields such as quantum chemistry [20, 28] and heuristic optimization [29, 30].

Furthermore, such variational quantum algorithms also offer a promising platform for the field of Machine Learning, which largely depends on training models to fit datasets and making predictions. Quantum Machine Learning (QML) algorithms have been developed for solving classification [31] and regression [6] tasks; the techniques include quantum versions of kernel methods [32, 33], support vector machines [34, 35], generative adversarial networks [36, 37], Born machines [38], Boltzmann machines [39], quantum neural networks [6, 40, 41] and more [26].

One regression task, fitting a continuous function  $f(x)$  to a dataset of scalar-valued points  $(x_i, y_i)$  in  $k$ -dimensional space, was analyzed for example in [6]. A quantum neural network, consisting of a quantum feature map circuit, a variational quantum circuit and a Hamiltonian operator was used to represent a parameterizable function  $f(x)$  that could be evaluated after training using gradient descent on analytically computed gradients of the loss function with respect to the variational circuit parameters.

In Ref. [15], Differentiable Quantum Circuits (DQCs) paradigm was introduced. A DQC implements a quantum neural network that can be analytically differentiated with respect to variational parameters *and* with respect to the network inputs. With automatic differentiation w.r.t. inputs it became possible to solve differential equations in a variational approach. In the current contribution, we will briefly summarize how this is done and we draw more parallels to classical scientific machine learning.

**Physics-Informed Machine Learning** Physics informed neural networks (PINNs) comprise a recent technique in scientific machine learning of particular relevance to this current work, since they bear strong conceptual similarities to DQCs. We see both DQCs and PINNs as universal function approximators (UFAs) which can be differentiated with respect to their inputs. Furthermore, both can be optimized so that such derivatives can be manipulated. Consequently, we expect that future applications of PINNs may well translate naturally to a DQC setting. Indeed, part of this current work is to demonstrate how such cross-fertilization between the fields might take place.

Introduced in [42], the essence of PINNs is to use (higher-order) derivatives of neural network outputs with respect to neural network inputs as terms with which to train neural networks. Consequently, neural networks can be trained to satisfy a given differential equation. Recently published work [2] has caused a surge in popularity of PINNs. For example, applications of PINNs have been found in diverse fields such as aerodynamic flow modelling [3] and cardiac activation mapping [43]. Apart from solving forward problems, they have also found use in solving inverse problems [3] and optimal control [44]. See [45] for a more complete recent review of PINNs and their applications.

Due to the conceptual similarity between PINNs and DQCs, we anticipate ample scope for cross-pollination of ideas and techniques between these lines of research. Of particular relevance to this current work is the application of PINNs to equation discovery [46], which we cover in more detail in subsequent sections.

**Classical Equation Discovery** A popular technique in equation discovery is to overparameterize a candidate differential equation solution in terms of a library of potential terms, and then fit to data while encouraging sparsity in differential equation coefficients [5] through an appropriate regularization term. The resulting non-zero coefficients provide an interpretable differential equation representation of a process which fits the data. While popularized in the context of ordinary differential equations (ODEs) [5], such techniques have been extended to the context of partial differential equations (PDEs) [47].

Such sparsity-driven equation discovery schemes have recently been introduced to PINNs [46]. We are not aware of any approaches to equation discovery which leverage quantum computation. Given the conceptual similarity between PINNs and DQCs, it is natural to extend such equation discovery techniques to a quantum setting, which is the purpose of this work.

Before we introduce our approach to *quantum model discovery* (QMoD [48]) in Sec. 2.4 we briefly introduce the DQC strategy that uses *quantum* neural networks as universal function approximators in Sec. 2.1.

**Our Contributions.** Our main contribution is to extend DQCs to wider applications in scientific machine learning, namely:

- parameter inference in differential equations
- discovery of unknown differential equations from empirical measurements

We demonstrate our approaches on two exemplary ordinary differential equations (ODE) and on one partial differential equation (PDE).

## 2 Methods

Differential equations lie at the heart of many engineering disciplines. However, using traditional, mesh-based methods such as finite-differencing or finite-elements do not lend themselves well to

several important applications, such as optimal control or solving inverse problems, since such applications require many repeated simulations. Therefore, it is desirable to find cost-effective alternatives such as data-driven differentiable surrogate models which can be optimized via gradient-based means. On classical hardware one way of obtaining differentiable surrogates that respect physical prior information is via *physics-informed neural networks* (PINNs). They can be used to solve PDEs given an equation, boundary conditions, and (optionally) some measurements. Our work builds on top of the quantum PINN analogue [15] which we briefly describe in Sec. 2.2.

We then demonstrate how further scientific machine learning techniques can be extended to a quantum setting. In Sec. 2.3, we introduce quantum methods for parameter inference in differential equations. Sec. 2.4 describes how to *discover* equations from measurements on quantum computers. By discovering we mean finding a unknown differential equation only from a given dataset and a pre-determined (large) library of possible terms.

## 2.1 Differentiable Quantum Universal Function Approximators

In DQC, quantum neural networks act as differentiable universal function approximators. These are quantum circuits consisting of three components: a quantum feature map, a variational ansatz, and a Hamiltonian operator for readout/encoding of the function. These elements act on an array of qubits and alter the system wavefunction in a specific way.

The feature map encodes the input variable  $x$  using a predefined non-linearity  $\varphi$  to the amplitudes of a quantum state  $\hat{\mathcal{U}}_\varphi(x)|0\rangle^n$ , where  $|0\rangle$  is some initially prepared state. In the simplest case this can be implemented with a single layer of rotations

$$\hat{\mathcal{U}}_\varphi(x) = \bigotimes_{j=1}^n \hat{R}_{\alpha,j}(\varphi_j(x)). \quad (1)$$

Furthermore, as an example, choosing the non-linearity as

$$\varphi_j(x) = j \cdot \arccos(x) \quad (2)$$

results in a Chebyshev basis in the amplitudes of  $\hat{\mathcal{U}}_\varphi(x)|0\rangle^n$ . The state now represents a basis of  $n$  Chebyshev polynomials which can be read out by measuring for example in the Z basis on each qubit. With a subsequent variational circuit (with parameters  $\theta$ ) the Chebyshev basis functions are combined; in the limit of large and controlled entanglement, such a setup allows access to up to  $\mathcal{O}(2^n)$  Chebyshev polynomials, due to the chaining and nesting properties of products of these polynomials. Similar effects occur for Fourier-type feature maps and other universal basis function sets. A popular choice for  $\hat{\mathcal{U}}_\theta$  is the so-called hardware efficient ansatz (HEA) with parameterized rotations and CNOT gates between neighboring qubits on the device.

The output  $\hat{u}(x, \theta)$  of the circuit is then computed with a Hamiltonian operator of choice,  $\hat{\mathcal{C}}$ , such that the final universal approximator for a scalar input variable  $x$  and variational parameters  $\theta$  then reads

$$\hat{u}(x, \theta) = \langle 0^n | \hat{\mathcal{U}}_\varphi^\dagger(x) \hat{\mathcal{U}}_\theta^\dagger \hat{\mathcal{C}} \hat{\mathcal{U}}_\theta \hat{\mathcal{U}}_\varphi(x) | 0^n \rangle \quad (3)$$

Under some conditions, equation 3 is fully analytically differentiable via the parameter shift rule [6] which requires two evaluations of the same circuit with shifted angles for each circuit-level parameter. As a particular example, where the feature map consists of single-qubit rotations, we can write the

derivative w.r.t.  $x$  as follows

$$\frac{d}{dx}\hat{u}(x, \theta) = \frac{1}{2} \frac{d\varphi}{dx} (\langle \hat{\mathcal{C}} \rangle^+ - \langle \hat{\mathcal{C}} \rangle^-), \quad (4)$$

$$\langle \hat{\mathcal{C}} \rangle^\pm = \sum_{j'} \langle 0^n | \hat{\mathcal{U}}_{\varphi, j, j'}^\pm(x) \hat{\mathcal{U}}_\theta^\dagger \hat{\mathcal{C}} \hat{\mathcal{U}}_\theta \hat{\mathcal{U}}_{\varphi, j, j'}^\pm(x) | 0^n \rangle, \quad (5)$$

$$\hat{\mathcal{U}}_{\varphi, j, j'}^\pm(x) = \bigotimes_{j=1}^n R_{y, j}(\varphi(x) \pm \frac{\pi}{2} \delta_{j, j'}). \quad (6)$$

Please note that we so-far considered a single-dimensional independent variable  $x$ . However, the DQC technique can straightforwardly be extended to multiple variables  $x, y, t$  etc by using multiple feature maps, one for each variable, and differentiating only those feature maps relevant to the variable differentiation of interest. An example application where this is shown in Ref. [49].

Furthermore, the example shows the regular parameter shift rule, which only applies to involutory quantum generators in the feature map. Generalized parameter shift rules exist for arbitrary generators, and hence for arbitrary feature map circuits [14]. In some cases, more intricate feature maps can be highly beneficial for increased expressivity of the quantum universal approximator.

## 2.2 Solving Differential Equations

We begin by recapping how to use automatically differentiable universal function approximators (either quantum or classical) to solve partial differential equations. This section unifies existing treatment of using neural networks to solve differential equations [2] and analogous quantum methods [15]. We write a partial differential equation in the form

$$F(u, \partial_t u, \partial_x u, \partial_x^2 u, \dots, x, t) = 0, \quad (7)$$

where  $x$  and  $t$  are dependent variables and  $u(x, t)$  is the solution we seek. For simplicity we will further refer to the LHS of equation 7 as  $F(u, x, t)$  omitting terms like  $\partial_x u$  or  $\partial_t u$  which in principle are operators acting on  $u$ . Let's imagine we had access to a trial function  $u(x, t)$  and we would like to ask how well it solves the differential equation system. To find the quality of an approximate solution  $\hat{u}(x, t, \theta)$  parameterized by  $\theta$  we can formulate a loss function

$$\mathcal{L}(\theta) = \mathcal{L}_F + \mathcal{L}_\Omega, \quad (8)$$

where  $\mathcal{L}_F$  is derived from the differential equation 7

$$\mathcal{L}_F = \frac{1}{M} \sum_{i=1}^M \|F(\hat{u}, x_i, t_i)\|_2. \quad (9)$$

and is thus minimized  $F(u, x, t) = 0$ , i.e. when  $\hat{u}(x, t, \theta)$  satisfies the partial differential equation dynamics. The second loss term  $\mathcal{L}_\Omega$  includes all boundary conditions which have to be met in order to fully specify the DE.

In order to effectively train such a model we ideally would like a universal approximator  $\hat{u}$  and access to its higher order derivatives both with respect to inputs  $x$  and  $t$ , as well as parameters  $\theta$ . Recent advances in automatic differentiation [50] have facilitated this using neural networks on classical hardware. On quantum hardware we leverage *differentiable quantum circuits* (DQC) [15] which implement a universal approximator based on a quantum featuremap  $\hat{\mathcal{U}}_\varphi(x)$  and a variational circuit  $\hat{\mathcal{U}}_\theta$ .

### 2.3 Inferring Differential Equation Parameters

As a first demonstration of how scientific machine learning can translate to novel quantum algorithms, we consider parameter inference in differential equations. In many situations, an overall structure of a differential equation is known, but specific coefficients must be inferred from data. For example, one might parameterize a given differential equation of some scalar variable  $u$  with some parameters  $\mathbf{w}$  to be identified:

$$F_{\mathbf{w}}(u, x, t) = 0, \quad (10)$$

where  $F = \mathbf{w}_1 \partial_x^2 u(x, t) + \mathbf{w}_2 x$  is one example, and the coefficients  $\mathbf{w}$  must be inferred from some given data set. We denote a given set of  $N$  data points with  $\{(x_i, t_i, y_i) : i = 1, 2 \dots N\}$ , where  $x_i$  and  $t_i$  denote independent variables and  $y_i$  is a scalar dependent variable. We assume that  $F$  is constructed so that there is no  $\mathbf{w}$  such that  $F = 0$  for every choice of  $u$  to avoid trivial solutions.

For example, to infer a one-dimensional diffusion coefficient one might define  $F$  as follows:

$$F_{\mathbf{w}} = \mathbf{w} \partial_x^2 u - \partial_t u, \quad (11)$$

where we have been mindful not to introduce a trainable coefficient to  $\partial_t u$ , which would allow (10) to be satisfied trivially with coefficients as zero.

To infer parameters in such settings, we introduce a loss function

$$\mathcal{L}(\boldsymbol{\theta}, \mathbf{w}) = \mathcal{L}_F + \mathcal{L}_d. \quad (12)$$

Note that unlike (8), we do not include a term analogous to  $\mathcal{L}_\Omega$  to represent boundary conditions. Although such terms could be introduced if boundary conditions are known, in principle the dynamics of the interior of the domain are inferrable from the data alone, and consequently boundary effects are not necessarily important to include.

In this loss function,

$$\mathcal{L}_F = \frac{1}{M} \sum_{i=1}^M \|F_{\mathbf{w}}(\hat{u}, x_i, t_i)\|_2 \quad (13)$$

ensures that the relevant differential equation dynamics are captured and

$$\mathcal{L}_d = \frac{1}{N} \sum_{i=1}^N \|\hat{u}(x_i, t_i, \boldsymbol{\theta}) - y_i\|_2 \quad (14)$$

provides incentive for the empirical dataset to be fit.

Note that we treat the loss function as a function of both the variational parameters,  $\boldsymbol{\theta}$ , as well as the inferred parameters,  $\mathbf{w}$ . In our experiments, we optimize both these parameters on an equal footing, i.e. they are trained with the same learning rate and same optimizer, but in principle a more general optimization scheme also suffices.

### 2.4 Discovering Differential Equations

Instead of solving a *known* differential equation this section describes how to find an *unknown* DE just from measurements and a library of plausible basis functions.

As in section 2.3, we start by introducing a parameterized differential equation which can be represented in a general form

$$F(u, x, t) = 0, \quad (15)$$



where again the coefficients  $\mathbf{w}$  must be inferred from some given data set. However, we parameterize  $F$  such that it represents a large family of PDEs of which we expect a given instance to fit the observed data. In particular, in the context of this work, we draw our attention to dynamical systems of the form

$$\partial_t u = \mathbf{w} \cdot \boldsymbol{\varphi}(u), \quad (16)$$

where  $u$  is a scalar dependent variable and  $\boldsymbol{\varphi}(u)$  is a library of potentially important functions such as

$$\boldsymbol{\varphi}(u) = [1, x, t, u, u^2, u^3, \partial_x u, \partial_x^2 u, u \partial_x u, \dots]^T. \quad (17)$$

The library  $\boldsymbol{\varphi}$  can be large if there is little prior knowledge about the terms that are present in the data, or contain only few specific terms that are likely to have generated the given dataset. Finding a solution that is *sparse* in  $\mathbf{w}$  results in a simple expression for the right-hand side (RHS) of equation 16. Hence, we can perform equation discovery by finding a sparse coefficient vector  $\mathbf{w}$ .

Equation 16 can be solved via STRidge regression ([5]) if one has access to measurements of both  $u$  and  $\partial_t u$  which is rare<sup>1</sup>. *Physics-informed neural networks* (PINN by [2]) which are normally used for *solving* DEs can circumvent this problem by learning a surrogate  $\hat{u}$  as described in Sec. 2.2. The surrogate is fully differentiable and therefore gives easy access to the derivatives needed to solve equation 16. Combining PINNs and equation 16 to DeepMoD ([46]) results in a fully automated framework that can discover DEs purely from data and a pre-specified library of basis functions  $\boldsymbol{\varphi}(u)$ . On classical hardware neural networks are used to represent the approximate solution  $\hat{u}$ . To perform equation discovery on NISQ devices we replace the classical neural networks with quantum universal function approximators implemented on DQCs resulting in our *Quantum Model Discovery* (QMoD) approach [48]. This approach is schematically depicted in figure 1.

The QMoD loss is composed of three terms: the data-loss  $\mathcal{L}_d$ , the DE (or physics) loss  $\mathcal{L}_p$ , and the regularization:

$$\mathcal{L}(\boldsymbol{\theta}, \mathbf{w}) = \lambda_d \mathcal{L}_d + \lambda_p \mathcal{L}_p + \lambda_r \|\mathbf{w}\|_1. \quad (18)$$

Note, that like equation 12, we do not include a term to impose boundary conditions. If boundary conditions are known, such a term might be introduced. However, we focus on situations where the interior PDE dynamics are inferred from data alone. Also, as in equation 12, we explicitly write the loss in terms of the variational parameters of the UFA ( $\boldsymbol{\theta}$ ), and the coefficients of the learnt differential equation ( $\mathbf{w}$ ). We optimize over both these parameters on an equal footing, using the same optimizer and learning rate. The term  $\lambda_r \|\mathbf{w}\|_1$  encourages sparsity in the solutions of  $\mathbf{w}$  and is standard practice in statistical learning [52].

The data-loss is the standard mean squared error (MSE)

$$\mathcal{L}_d = \frac{1}{N} \sum_{i=1}^N \|\hat{u}(x_i, t_i, \boldsymbol{\theta}) - y_i\|_2, \quad (19)$$

running over  $N$  data points with temporal, spatial and scalar responses given by  $t_i$ ,  $x_i$  and  $y_i$  respectively. The differential equation loss is computed via the linear combination of basis functions

$$\mathcal{L}_p = \frac{1}{M} \sum_{i=1}^M \|\partial_t \hat{u}(x_i, t_i, \boldsymbol{\theta}) - \mathbf{w} \boldsymbol{\varphi}(\hat{u})\|_2. \quad (20)$$

The points  $(x_i, t_i)$  at which the DE loss is evaluated can be chosen independently from the data grid of equation 19 via a fixed, random, or adaptive grid which gives this method great flexibility.

---

<sup>1</sup>If measurements of  $\partial_t u$  are not directly available they can be computed e.g. via the Savitzky-Golay filter ([51]), but such methods typically require very dense measurements.



Generalizing QMoD to higher dimensional  $\mathbf{u} = [u_1, u_2, \dots]^T$  only requires taking care of matching dimensions (e.g. the coefficient vector  $\mathbf{w}$  turns into a matrix). In the equation discovery setting it makes sense to prevent the surrogates for the variables  $u_i$  from interaction, because we want the interaction of terms to occur only via the library  $\varphi$ . Therefore, we use one individual UFA per operator instead of one large UFA with multiple outputs, that would allow interaction outside the library.

### 3 Experiments

In this section, we demonstrate quantum scientific machine learning to be a viable technique. In addition to demonstrating parameter inference, we also compare our QMoD to its classical, neural network based counter part (DeepMoD). We generate data from several different differential equations and demonstrate applications of QMoD.

#### 3.1 Damped Harmonic Oscillator

We start by demonstrating the potential of quantum neural networks for parameter inference and equation discovery in second-order ODES.

We parameterize a damped harmonic oscillator as follows:

$$\frac{d^2 u_d}{dt_d^2} = -\omega^2 u_d - \alpha \frac{du_d}{dt_d}, \quad (21)$$

where  $u_d$  is the position,  $\omega$  the frequency, and  $\alpha$  the damping coefficient of the oscillator. The index  $d$  indicates that this is the ODE before non-dimensionalization. We non-dimensionalize the equation such that the data lies in within the range  $(-1, 1)$  by defining  $u_d = uu_c$  and  $t_d = tt_c$  which results in

$$\frac{d^2 u}{dt^2} = -\omega^2 t_c^2 u - \alpha t_c^2 \frac{du}{dt}, \quad (22)$$

With the constants  $u_c = 1$  m,  $t_c = 2\pi$  s,  $\omega = 1.5 \frac{1}{s}$ , and  $\alpha = 0.5 \frac{1}{s}$  we obtain training data as shown on the left plot of figure 2.

##### 3.1.1 Inferring Differential Equation Parameters

As a first step we assume that the form the governing differential equation is known and we must infer the values of the constants  $\omega$  and  $\alpha$ . We compare the method outlined in section 2.3 with an implementation of DeepMoD without regularization coefficients. The optimization problem in (12) with the specialized form of (10) is defined as:

$$F_{\mathbf{w}}(u, x, t) = \frac{d^2 u}{dt^2} + \mathbf{w} \left[ t_c^2 u, t_c^2 \frac{du}{dt} \right]^T. \quad (23)$$

We include the known non-dimensionalization constants in the basis functions to scale the problem so that it is more amenable to standard optimization hyperparameters (not doing this would result in the models having to identify coefficients  $\gg 10$ ).

Figure 2 shows the data and the obtained QMoD fit  $\hat{u}$  on the left. We use a quantum neural network with 5 qubits as the UFA to approximate  $\hat{u}$ . We reach an MSE loss value of  $\mathcal{L}_d = 10^{-7}$  after 200 BFGS optimization steps. A neural network with one hidden layer of size 32 and tanh activations reaches similar MSE. The central and right plot of figure 2 show the trajectories of the coefficients of

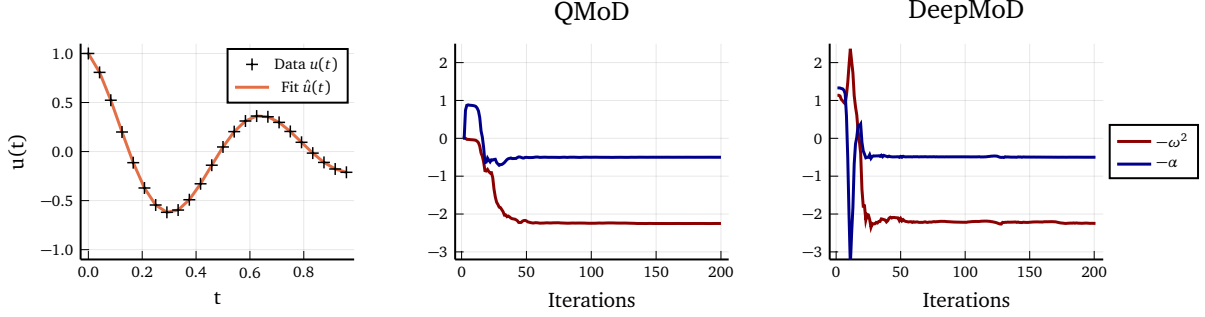


Figure 2: Damped harmonic parameter *identification*. *Left*: Quantum UFA fit to the training data. *Center & right*: Trajectories of QMoD & DeepMoD basis function coefficients ( $w_i$ ) during training. Both QMoD and the classical DeepMoD infer the correct target parameters  $\omega^2 = 2.25$  and  $\alpha = 0.5$ .

Equation	Model	Basis function	
		$u$	$\frac{du}{dt}$
$\frac{d^2u}{dt^2} = -\omega^2 t_c^2 u - \alpha t_c^2 \frac{du}{dt}$	QMoD	$\omega = \sqrt{2.249} = 1.499$	$\alpha = 0.500$
	DeepMoD	$\omega = \sqrt{2.247} = 1.498$	$\alpha = 0.500$
	Truth	$\omega = 1.5$	$\alpha = 0.5$

Table 1: Final basis function parameters  $\omega$  and  $\alpha$  as inferred by QMoD and DeepMoD compared to the true coefficients that generated the data (called *truth*). Non-dimensionalization coefficients in the basis functions are omitted for clarity.

the two basis functions (equation 23), namely  $\omega$  and  $\alpha$ , during training. The target values for the two coefficients are  $\omega = 1.5$  and  $\alpha = 0.5$ .

In this experiment we found good solutions using  $\lambda_d = 1$  (dataloss),  $\lambda_p = 10^{-5}$  (physics loss) for both QMoD and DeepMoD within (12). The identified parameter values are shown in table 3.1.1.

### 3.1.2 Equation Discovery

To go a step beyond the task of parameter inference, we next aim for full "equation discovery"; we assume that only the LHS of equation 22 (i.e.  $\partial u_t^2$ ) is known and choose a set of plausible basis functions  $\varphi$  consisting of polynomials up to degree 4 and the first derivative of  $u$  for use in (16).

$$\varphi(u) = \left[ t_c^2 u(t), \quad u_c t_c^2 u^2(t), \quad u_c^2 t_c^2 u^3(t), \quad u_c^3 t_c^2 u^4(t), \quad t_c \frac{du}{dt} \right]^T \quad (24)$$

We optimize (18) and achieve good results with a regularization parameter  $\lambda_r = 10^{-4}$ . Otherwise we use the same training and model setup (5 qubits, 200 BFGS steps,  $\lambda_p = 10^{-5}$ ) as in section 3.1.1. Both our quantum equation discovery QMoD and DeepMoD successfully identify the relevant basis functions and their correct coefficients. All other basis function coefficients are close to zero after training.

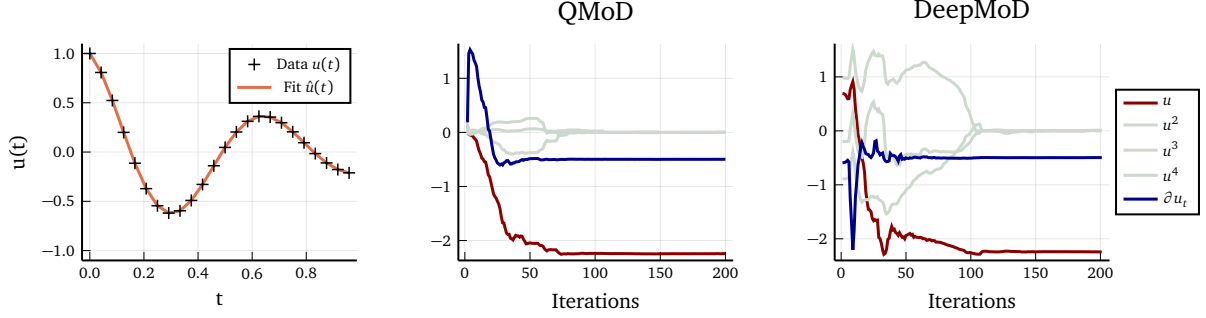


Figure 3: Damped harmonic oscillator *discovery*. *Left*: Quantum UFA fit to the training data. *Center & right*: Trajectories of QMoD & DeepMoD basis function coefficients ( $w_i$ ) during training. The difference to figure 2 is the larger set of basis functions. Both QMoD and DeepMoD correctly identify the relevant basis functions ( $u$  and  $\frac{du}{dt}$ ) whereas the irrelevant basis function coefficients are all close to zero.

Equation	Model	Basis function				
		$u$	$u^2$	$u^3$	$u^4$	$\frac{du}{dt}$
$\frac{d^2u}{dt^2} = -\omega^2 t_c^2 u - \alpha t_c^2 \frac{du}{dt}$	QMoD	$\omega = \sqrt{2.239} = 1.496$	$< 10^{-3}$	$< 10^{-3}$	$< 10^{-3}$	$\alpha = 0.497$
	DeepMoD	$\omega = \sqrt{2.242} = 1.498$	$< 10^{-3}$	$< 10^{-3}$	$< 10^{-3}$	$\alpha = 0.496$
	Truth	$\omega = 1.5$	0	0	0	$\alpha = 0.5$

Table 2: Final basis function parameters resulting from QMoD/DeepMoD training with a larger library of basis functions (equation 24). All irrelevant coefficients are very close to zero while the inferred  $\omega$  and  $\alpha$  are close to their true values. Non-dimensionalization coefficients in the basis functions are omitted for clarity.

### 3.2 Lotka-Volterra System

We now demonstrate that coupled non-linear differential equations can be discovered with quantum circuits. Our model system is given by the Lotka-Volterra (LV) equations:

$$\frac{dx_d}{dt_d} = \alpha x_d - \beta x_d y_d \quad (25)$$

$$\frac{dy_d}{dt_d} = \delta x_d y_d - \gamma y_d \quad (26)$$

that describe a predator-prey system where  $x_d$  is the number of prey and  $y_d$  the number of predators. The parameters  $\alpha$ ,  $\beta$ ,  $\gamma$ , and  $\delta$  define the interaction of the two species which we chose to  $\alpha = 1.5$ ,  $\beta = 1$ ,  $\gamma = 1$ ,  $\delta = 1$ . Again, the index  $d$  indicates dimensional quantities. We non-dimensionalize the LV system with critical time  $t_c = 8$  and a critical number of individuals  $x_c = 2.5$  which results in

$$\frac{dx}{dt} = \alpha t_c x - t_c x_c \beta x y \quad (27)$$

$$\frac{dy}{dt} = t_c x_c \delta x y - t_c \gamma y. \quad (28)$$

The non-dimensionalization coefficients are again included in the basis functions  $\varphi$  which consist of polynomials up to degree 2

$$\varphi(x, y) = [t_c x, t_c y, t_c x_c x^2, t_c x_c y^2, t_c x_c x y]^T. \quad (29)$$

QMoD is trained with a time-series of 30 datapoints for each variable  $x$  and  $y$ . For this task we need a slightly larger featuremap with 7 qubits to fit the data. Each variable of the LV system is modeled by a separate UFA driving its own set of (identical) library functions. After 200 BFGS steps we discover the correct basis function coefficients as shown in figure 4 and table 3.2. The QMoD loss coefficients are  $\lambda_d = 1$ ,  $\lambda_p = 10^{-3}$ , and  $\lambda_r = 10^{-5}$ .

We compare QMoD to classical DeepMoD with two neural networks (one for each variable  $x$  and  $y$ ) with one hidden layer of size 32. Classical DeepMoD receives the same data. For this dataset we observe that the classical neural networks suffer from stronger gradient pathologies which could only be resolved by decreasing the physics loss coefficient to  $\lambda_p = 10^{-6}$  which weakens the training signal on the basis function coefficients. This explains why DeepMoD needs more training steps to converge (see figure 4).

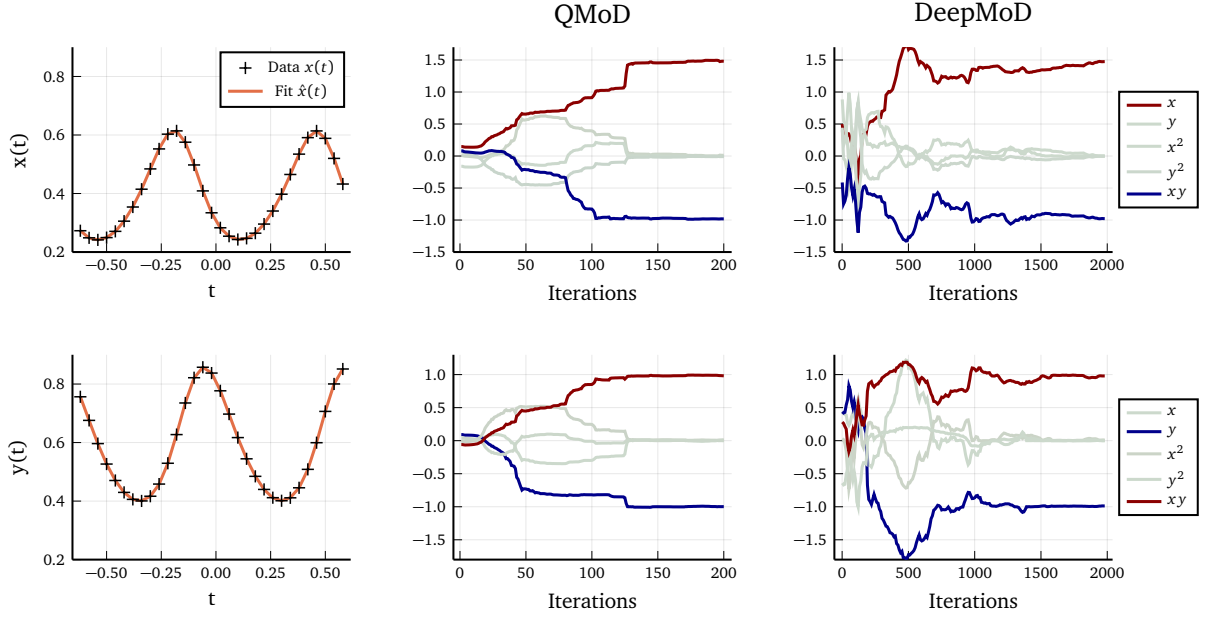


Figure 4: Lotka-Volterra discovery. *Left*: Quantum UFA fit to the training data. *Center & right*: Trajectories of QMoD & DeepMoD basis function coefficients ( $w_i$ ) during training. Both QMoD and DeepMoD correctly identify the relevant basis functions for each variable.

Equation	Model	Basis function				
		$x$	$y$	$x^2$	$y^2$	$xy$
$\frac{dx}{dt} = \alpha t_c x - t_c x_c \beta xy$	QMoD	$\alpha = 1.483$	0.001	-0.001	-0.007	$\beta = 0.986$
	DeepMoD	$\alpha = 1.475$	$< 10^{-3}$	$< 10^{-3}$	-0.003	$\beta = 0.979$
	Truth	$\alpha = 1.5$	0	0	0	$\beta = 1$
$\frac{dy}{dt} = t_c x_c \delta xy - t_c \gamma y$	QMoD	0.006	$\delta = 0.993$	0.008	$< 10^{-3}$	$\gamma = 0.991$
	DeepMoD	$< 10^{-3}$	$\delta = 0.987$	0.011	$< 10^{-3}$	$\gamma = 0.979$
	Truth	0	$\delta = 1$	0	0	$\gamma = 1$

Table 3: Final basis function parameters of the LV system discovered by QMoD and DeepMoD compared to the true coefficients that generated the data (called *truth*). Non-dimensionalization coefficients in the basis functions are omitted for clarity. Both models identify the correct basis functions as relevant.

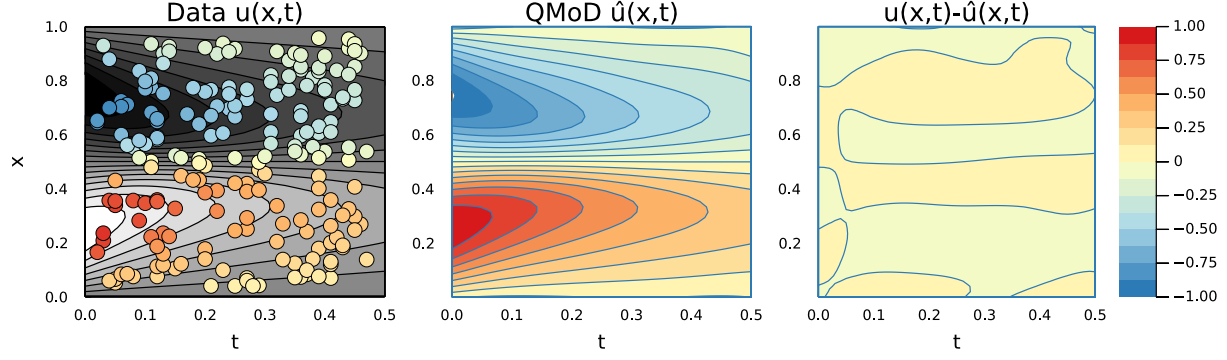


Figure 5: *Left*: Scatter plot of Burgers' equation dataset and the full solution as a gray-scale contour underneath (parameters  $\varepsilon = 0.05$ ,  $\alpha = 1$ , and initial condition  $u(x, 0) = \sin(2\pi x)$ ). *Center*: Learned QMoD solution. *Right*: Error of QMoD solution.

### 3.3 Burgers' Equation

In this last section we present the discovery of Burgers' equation, a non-linear second-order partial differential equation. We chose the general (or *viscous*) Burgers equation with one spatial dimension  $x$  and one time dimension  $t$ :

$$\frac{\partial u}{\partial t} = \varepsilon \frac{\partial^2 u}{\partial x^2} - \alpha u \frac{\partial u}{\partial x}, \quad (30)$$

where  $u(x, t)$  is the velocity field,  $\varepsilon$  the viscosity, and  $\alpha$  the coefficient of the advection term. To obtain training data we solve Burgers' equation on the domain  $(x \times t) \in ([0, 1] \times [0, \frac{1}{2}])$  with parameters  $\varepsilon = 0.05$  and  $\alpha = 1$ . The true solution with sinusoidal initial conditions

$$u(x, 0) = \sin(2\pi x) \quad (31)$$

is shown in the left plot of figure 5 as the gray-scale contour. We train on 200 uniformly sampled points<sup>2</sup> which are scattered on top of the left plot of figure 5. For Burgers' equation we do not need to perform non-dimensionalization as the domain is already within  $(-1, 1)$ . We assume that the LHS  $\partial u_t$  is known and want to discover  $\varepsilon$  and  $\alpha$  from the library

$$\varphi(u) = \left[ u, \quad u^2, \quad \frac{\partial u}{\partial x}, \quad \frac{\partial^2 u}{\partial x^2}, \quad u \frac{\partial u}{\partial x}, \quad u^2 \frac{\partial u}{\partial x} \right]^T. \quad (32)$$

To solve this PDE we need a UFA with two inputs  $(x, t)$  and one output. Therefore, we employ two input featuremaps with 6 qubits each. The two featuremaps are stacked in parallel onto one circuit, and connected to a variational circuit with a base on all 12 qubits, effectively entangling the two feature registers. The physics loss coefficient is set to  $\lambda_p = 10^{-2}$  and the regularization to  $\lambda_r = 10^{-3}$ . Figure 6 and table 3.3 show that  $\varepsilon$  is discovered very precisely but the advection term  $\alpha$  is slightly too low in both models. However, we can still conclude that QMoD and DeepMoD correctly identify the two relevant basis functions for advection and diffusion. To get an even closer fit to the true basis function parameters it is possible to re-run the model only with the two relevant basis functions and switch off the regularization (as we demonstrated in section 3.1.1).

<sup>2</sup>Note that no intricate grid definition is needed for DQC/QMoD to solve PDEs

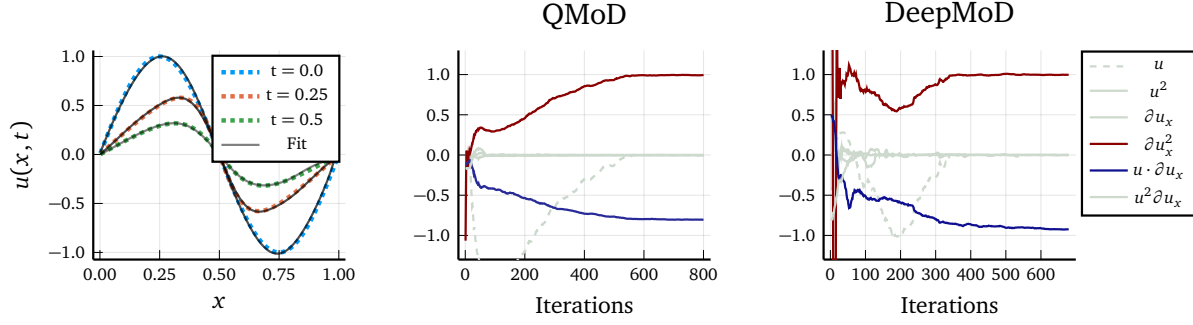


Figure 6: Burgers' equation discovery. *Left*: Quantum UFA fit to the training data. *Center & right*: Trajectories of QMoD & DeepMoD basis function coefficients ( $w_i$ ) during training. The trajectory of viscosity  $\epsilon$  (red line) is scaled by  $\frac{1}{\epsilon}$  for better visibility. Both QMoD and DeepMoD discover  $\epsilon$  with good precision. The advection term  $\alpha$  (blue line) is clearly discovered as a relevant term but does not match the true value  $\alpha = 1$  perfectly.

Equation	Model	Basis function					
		$u$	$u^2$	$\frac{du}{dx}$	$\frac{d^2u}{dx^2}$	$u \frac{du}{dx}$	$u^2 \frac{du}{dx}$
$\frac{\partial u}{\partial t} = \epsilon \frac{\partial^2 u}{\partial x^2} - \alpha u \frac{\partial u}{\partial x}$	QMoD	$< 10^{-3}$	$< 10^{-3}$	$< 10^{-3}$	$\epsilon = 0.050$	$\alpha = 0.838$	$< 10^{-3}$
	DeepMoD	$< 10^{-3}$	$< 10^{-3}$	$< 10^{-3}$	$\epsilon = 0.049$	$\alpha = 0.924$	$< 10^{-3}$
	Truth	0	0	0	$\epsilon = 0.05$	$\alpha = 1$	$< 10^{-3}$

Table 4: Final basis function parameters for Burgers' equation discovered by QMoD and DeepMoD compared to the true coefficients that generated the data. Both QMoD and DeepMoD correctly identify that only two basis functions are needed to describe Burgers' equation. The parameters  $\epsilon$  is found very precisely by both models. DeepMoD is closer to the true parameter  $\alpha$  but still slightly too low.



## 4 Discussion & Conclusion

We demonstrated that techniques from scientific machine learning can be placed in a quantum computational setting. In particular, our numerical experiments show that relatively small quantum circuits can be used for meaningful computations in scientific machine learning. We have demonstrated how to implement an automated parameter inference and equation discovery framework (QMoD) using a differentiable quantum circuit strategy, and reached results that are on par with the classical machine learning method DeepMoD. With this demonstration of what can be achieved with DQCs the fields of quantum computing and scientific machine learning are moving closer together.

We should note that all experiments described here involve classical simulators of quantum computers with unrealistic assumptions such as zero sampling noise, no environment noise and no measurement noise. Although many error mitigation strategies for NISQ hardware exist, it should still be investigated how well the strategies described work in more realistic settings and importantly on real quantum hardware, and which quantum hardware is most compatible/natural for this strategy. Furthermore, due to the intrinsic scaling issues of simulating quantum many-body systems, we did not consider more than 12 qubits in the largest simulations described here, and thus also compared with only small-sized classical neural networks. It will be important to investigate the performance for larger number of qubits on quantum hardware, and compare them to realistic classical PINN architectures.

The strategies described above work for systems governed by sets of Partial Differential Equations, but also for those governed by stochastic processes modelled as Stochastic (Partial) Differential Equations (SDEs), through the perspective of *quantile mechanics* combined with DQCs as described in the recent paper on Quantum Quantile Mechanics (QQM) [49]. In such setting, an SDE may be learned (‘discovered’) based on just statistical data. This could prove valuable in the generative modelling case, where synthetic data generation of time-series is learned based on a combination of data and a parameterized SDE with a library of candidate model operators. In such real-world setting as financial markets, there is often not exact knowledge of the underlying model dynamics but there is access to historical data, where QMoD could infer the SDE from data and make better predictions compared to a purely data-only approach.

An interesting area of potential yet unexplored, is the identification of quantum computational speedup for scientific machine learning in other aspects than Neural Network enhancement, for example by combining QMoD with combinatorial optimization.

*Ethics declaration.* A patent application for the method described in this manuscript has been submitted by Qu&Co.

## References

- [1] Ricky T. Q. Chen et al. “Neural Ordinary Differential Equations”. In: *NeurIPS* 109. NeurIPS (June 2018), pp. 31–60. URL: <https://proceedings.neurips.cc/paper/2018/file/69386f6bb1dfed68692a24c8686939b9-Paper.pdf>.
- [2] Maziar Raissi, Paris Perdikaris, and G.E. Karniadakis. “Physics-informed neural networks: A deep learning framework for solving forward and inverse problems involving nonlinear partial differential equations”. In: *Journal of Computational Physics* 378 (Feb. 2019), pp. 686–707. ISSN: 00219991. DOI: [10.1016/j.jcp.2018.10.045](https://doi.org/10.1016/j.jcp.2018.10.045).
- [3] Zhiping Mao, Ameya D. Jagtap, and George Em Karniadakis. “Physics-informed neural networks for high-speed flows”. In: *Computer Methods in Applied Mechanics and Engineering* 360 (Mar. 2020), p. 112789. ISSN: 0045-7825. DOI: [10.1016/J.CMA.2019.112789](https://doi.org/10.1016/J.CMA.2019.112789).

- [4] Alexandre M. Tartakovsky et al. “Learning Parameters and Constitutive Relationships with Physics Informed Deep Neural Networks”. In: (Aug. 2018). URL: <https://arxiv.org/abs/1808.03398v2>.
- [5] Steven L. Brunton, Joshua L. Proctor, and J. Nathan Kutz. “Discovering governing equations from data by sparse identification of nonlinear dynamical systems”. In: *Proceedings of the National Academy of Sciences* 113.15 (Apr. 2016), pp. 3932–3937. ISSN: 0027-8424. DOI: [10.1073/pnas.1517384113](https://doi.org/10.1073/pnas.1517384113).
- [6] K. Mitarai et al. “Quantum circuit learning”. In: *Physical Review A* 98.3 (Sept. 2018). ISSN: 2469-9926. DOI: [10.1103/PhysRevA.98.032309](https://doi.org/10.1103/PhysRevA.98.032309).
- [7] Javier Gil Vidal and Dirk Oliver Theis. “Calculus on parameterized quantum circuits”. In: *arXiv* (Dec. 2018). URL: <http://arxiv.org/abs/1812.06323>.
- [8] Gavin E. Crooks. “Gradients of parameterized quantum gates using the parameter-shift rule and gate decomposition”. In: *arXiv* (May 2019). URL: <http://arxiv.org/abs/1905.13311>.
- [9] Maria Schuld et al. “Evaluating analytic gradients on quantum hardware”. In: *Physical Review A* 99.3 (Mar. 2019), p. 032331. ISSN: 2469-9926. DOI: [10.1103/PhysRevA.99.032331](https://doi.org/10.1103/PhysRevA.99.032331).
- [10] Andrea Mari, Thomas R. Bromley, and Nathan Killoran. “Estimating the gradient and higher-order derivatives on quantum hardware”. In: *Physical Review A* 103.1 (Jan. 2021), p. 012405. ISSN: 2469-9926. DOI: [10.1103/PhysRevA.103.012405](https://doi.org/10.1103/PhysRevA.103.012405).
- [11] Leonardo Banchi and Gavin E Crooks. “Measuring Analytic Gradients of General Quantum Evolution with the Stochastic Parameter Shift Rule”. In: *Quantum* 5 (Jan. 2021), p. 386. ISSN: 2521-327X. DOI: [10.22331/q-2021-01-25-386](https://doi.org/10.22331/q-2021-01-25-386).
- [12] M Cerezo and Patrick J Coles. “Higher order derivatives of quantum neural networks with barren plateaus”. In: *Quantum Science and Technology* 6.3 (July 2021), p. 035006. ISSN: 2058-9565. DOI: [10.1088/2058-9565/abf51a](https://doi.org/10.1088/2058-9565/abf51a).
- [13] Thomas Hubregtsen et al. “Single-component gradient rules for variational quantum algorithms”. In: *arXiv* (June 2021). URL: <http://arxiv.org/abs/2106.01388>.
- [14] Oleksandr Kyriienko and Vincent E Elfving. “Generalized quantum circuit differentiation rules”. In: *arXiv* (Aug. 2021). URL: <https://arxiv.org/abs/2108.01218>.
- [15] Oleksandr Kyriienko, Annie E Paine, and Vincent E Elfving. “Solving nonlinear differential equations with differentiable quantum circuits”. In: *Physical Review A* 103.5 (May 2021), p. 052416. ISSN: 2469-9926. DOI: [10.1103/PhysRevA.103.052416](https://doi.org/10.1103/PhysRevA.103.052416).
- [16] Gordon Moore. “Cramming more components onto integrated circuits, Reprinted from *Electronics*, volume 38, number 8, April 19, 1965, pp.114 ff”. In: *Electronics* 38.8 (1965), p. 114. DOI: [10.1109/N-SSC.2006.4785860](https://doi.org/10.1109/N-SSC.2006.4785860).
- [17] Thomas N Theis and H-S Philip Wong. “The End of Moore’s Law: A New Beginning for Information Technology”. In: *Computing in Science & Engineering* 19.2 (Mar. 2017), pp. 41–50. ISSN: 1521-9615. DOI: [10.1109/MCSE.2017.29](https://doi.org/10.1109/MCSE.2017.29).
- [18] A.V. Krishnamoorthy et al. “Computer Systems Based on Silicon Photonic Interconnects”. In: *Proceedings of the IEEE* 97.7 (July 2009), pp. 1337–1361. ISSN: 0018-9219. DOI: [10.1109/JPROC.2009.2020712](https://doi.org/10.1109/JPROC.2009.2020712).
- [19] Jerome Bonnet et al. “Amplifying Genetic Logic Gates”. In: *Science* 340.6132 (May 2013), pp. 599–603. ISSN: 0036-8075. DOI: [10.1126/science.1232758](https://doi.org/10.1126/science.1232758).

- [20] Abhinav Kandala et al. “Hardware-efficient variational quantum eigensolver for small molecules and quantum magnets”. In: *Nature* 549.7671 (2017), pp. 242–246. ISSN: 1476-4687. DOI: [10.1038/nature23879](https://doi.org/10.1038/nature23879).
- [21] Frank Arute et al. “Quantum supremacy using a programmable superconducting processor”. In: *Nature* 574.7779 (2019), pp. 505–510. ISSN: 14764687. DOI: [10.1038/s41586-019-1666-5](https://doi.org/10.1038/s41586-019-1666-5).
- [22] Peter W. Shor. “Polynomial-Time Algorithms for Prime Factorization and Discrete Logarithms on a Quantum Computer”. In: *SIAM Journal on Computing* 26.5 (Aug. 1995), pp. 1484–1509. DOI: [10.1137/S0097539795293172](https://doi.org/10.1137/S0097539795293172).
- [23] Lov K Grover. “A fast quantum mechanical algorithm for database search”. In: *Proceedings of the twenty-eighth annual ACM symposium on Theory of computing - STOC '96*. New York, New York, USA: ACM Press, 1996, pp. 212–219. ISBN: 0897917855. DOI: [10.1145/237814.237866](https://doi.org/10.1145/237814.237866).
- [24] Yudong Cao et al. “Quantum Chemistry in the Age of Quantum Computing”. In: *Chemical Reviews* 119.19 (Oct. 2019), pp. 10856–10915. ISSN: 0009-2665. DOI: [10.1021/acs.chemrev.8b00803](https://doi.org/10.1021/acs.chemrev.8b00803).
- [25] V E Elfving et al. “How will quantum computers provide an industrially relevant computational advantage in quantum chemistry?” In: *arXiv* (Sept. 2020). URL: <http://arxiv.org/abs/2009.12472>.
- [26] Jacob Biamonte et al. “Quantum machine learning”. In: *Nature* 549.7671 (Sept. 2017), pp. 195–202. ISSN: 0028-0836. DOI: [10.1038/nature23474](https://doi.org/10.1038/nature23474).
- [27] John Preskill. “Quantum Computing in the NISQ era and beyond”. In: *Quantum* (Jan. 2018). DOI: [10.22331/q-2018-08-06-79](https://doi.org/10.22331/q-2018-08-06-79).
- [28] Vincent E Elfving et al. “Simulating quantum chemistry in the seniority-zero space on qubit-based quantum computers”. In: *Phys. Rev. A* 103.3 (Mar. 2021), p. 32605. DOI: [10.1103/PhysRevA.103.032605](https://doi.org/10.1103/PhysRevA.103.032605).
- [29] Edward Farhi, Jeffrey Goldstone, and Sam Gutmann. “A Quantum Approximate Optimization Algorithm”. In: *arXiv* (2014). URL: <https://arxiv.org/abs/1411.4028>.
- [30] Ajinkya Borle, Vincent E. Elfving, and Samuel J. Lomonaco. “Quantum Approximate Optimization for Hard Problems in Linear Algebra”. In: *arXiv* (June 2020), pp. 1–12. URL: <http://arxiv.org/abs/2006.15438>.
- [31] Vojtěch Havlíček et al. “Supervised learning with quantum-enhanced feature spaces”. In: *Nature* 567.7747 (Mar. 2019), pp. 209–212. ISSN: 0028-0836. DOI: [10.1038/s41586-019-0980-2](https://doi.org/10.1038/s41586-019-0980-2).
- [32] Maria Schuld and Nathan Killoran. “Quantum machine learning in feature Hilbert spaces”. In: *Physical Review Letters* (Mar. 2018). DOI: [10.1103/PhysRevLett.122.040504](https://doi.org/10.1103/PhysRevLett.122.040504).
- [33] Maria Schuld. “Supervised quantum machine learning models are kernel methods”. In: *arXiv* (Jan. 2021). URL: <http://arxiv.org/abs/2101.11020>.
- [34] Patrick Rebentrost, Masoud Mohseni, and Seth Lloyd. “Quantum Support Vector Machine for Big Data Classification”. In: *Physical Review Letters* 113.13 (Sept. 2014), p. 130503. DOI: [10.1103/PhysRevLett.113.130503](https://doi.org/10.1103/PhysRevLett.113.130503).
- [35] Yunchao Liu, Srinivasan Arunachalam, and Kristan Temme. “A rigorous and robust quantum speed-up in supervised machine learning”. In: *Nature Physics* 17.9 (Sept. 2021), pp. 1013–1017. ISSN: 1745-2473. DOI: [10.1038/s41567-021-01287-z](https://doi.org/10.1038/s41567-021-01287-z).

- [36] Pierre-Luc Dallaire-Demers and Nathan Killoran. “Quantum generative adversarial networks”. In: *Physical Review A* (Apr. 2018). DOI: [10.1103/PhysRevA.98.012324](https://doi.org/10.1103/PhysRevA.98.012324).
- [37] Seth Lloyd and Christian Weedbrook. “Quantum generative adversarial learning”. In: *Physical Review Letters* (Apr. 2018). DOI: [10.1103/PhysRevLett.121.040502](https://doi.org/10.1103/PhysRevLett.121.040502).
- [38] Brian Coyle et al. “The Born supremacy: quantum advantage and training of an Ising Born machine”. In: *npj Quantum Information* 6.1 (Dec. 2020), p. 60. ISSN: 2056-6387. DOI: [10.1038/s41534-020-00288-9](https://doi.org/10.1038/s41534-020-00288-9).
- [39] Mohammad H. Amin et al. “Quantum Boltzmann Machine”. In: *Physical Review X* (Jan. 2016). DOI: [10.1103/PhysRevX.8.021050](https://doi.org/10.1103/PhysRevX.8.021050).
- [40] Marcello Benedetti et al. “Parameterized quantum circuits as machine learning models”. In: *Quantum Science and Technology* 4.4 (Nov. 2019), p. 043001. ISSN: 2058-9565. DOI: [10.1088/2058-9565/ab4eb5](https://doi.org/10.1088/2058-9565/ab4eb5).
- [41] Amira Abbas et al. “The power of quantum neural networks”. In: *Nature Computational Science* 1.6 (2021), pp. 403–409. ISSN: 2662-8457. DOI: [10.1038/s43588-021-00084-1](https://doi.org/10.1038/s43588-021-00084-1).
- [42] I.E. Lagaris, A. Likas, and D.I. Fotiadis. “Artificial neural networks for solving ordinary and partial differential equations”. In: *IEEE Transactions on Neural Networks* 9.5 (May 1998), pp. 987–1000. ISSN: 10459227. DOI: [10.1109/72.712178](https://doi.org/10.1109/72.712178).
- [43] Francisco Sahli Costabal et al. “Physics-Informed Neural Networks for Cardiac Activation Mapping”. In: *Frontiers in Physics* 0 (Feb. 2020), p. 42. ISSN: 2296-424X. DOI: [10.3389/FPHY.2020.00042](https://doi.org/10.3389/FPHY.2020.00042).
- [44] Sifan Wang, Mohamed Aziz Bhouri, and Paris Perdikaris. “Fast PDE-constrained optimization via self-supervised operator learning”. In: (Oct. 2021). URL: <https://arxiv.org/abs/2110.13297v1>.
- [45] George Em Karniadakis et al. “Physics-informed machine learning”. In: *Nature Reviews Physics* 2021 3:6 3.6 (May 2021), pp. 422–440. ISSN: 2522-5820. DOI: [10.1038/s42254-021-00314-5](https://doi.org/10.1038/s42254-021-00314-5).
- [46] Gert-Jan Both et al. “DeepMoD: Deep learning for model discovery in noisy data”. In: *Journal of Computational Physics* 428 (Mar. 2021), p. 109985. ISSN: 00219991. DOI: [10.1016/j.jcp.2020.109985](https://doi.org/10.1016/j.jcp.2020.109985). URL: <https://linkinghub.elsevier.com/retrieve/pii/S0021999120307592>.
- [47] Samuel H Rudy et al. “Data-driven discovery of partial differential equations”. In: *Science Advances* 3.4 (Apr. 2017). ISSN: 2375-2548. DOI: [10.1126/sciadv.1602614](https://doi.org/10.1126/sciadv.1602614).
- [48] *A patent application for the method described in this manuscript has been submitted by Qu&Co.*
- [49] Annie E Paine, Vincent E Elfving, and Oleksandr Kyriienko. “Quantum Quantile Mechanics: Solving Stochastic Differential Equations for Generating Time-Series”. In: *arXiv* (Aug. 2021). URL: <https://arxiv.org/abs/2108.03190>.
- [50] Atılım Güne, et al. *Automatic Differentiation in Machine Learning: a Survey*. Tech. rep. 2018, pp. 1–43.
- [51] Ronald W Schafer. “What Is a Savitzky-Golay Filter?” In: *IEEE Signal Processing Magazine* 28.4 (2011), pp. 111–117. DOI: [10.1109/MSP.2011.941097](https://doi.org/10.1109/MSP.2011.941097).
- [52] Trevor Hastie, Robert Tibshirani, and Jerome Friedman. *The Elements of Statistical Learning*. Springer Series in Statistics. New York, NY: Springer New York, 2009. ISBN: 978-0-387-84857-0. DOI: [10.1007/978-0-387-84858-7](https://doi.org/10.1007/978-0-387-84858-7).